Inductively Heated Shape Memory Polymer for the Magnetic Actuation of Medical Devices

Patrick R. Buckley*, Gareth H. McKinley, Thomas S. Wilson, Ward Small, IV, William J. Benett, Jane P. Bearinger, Michael W. McElfresh, and Duncan J. Maitland

Abstract—**Presently, there is interest in making medical devices such as expandable stents and intravascular microactuators from shape memory polymer (SMP). One of the key challenges in realizing SMP medical devices is the implementation of a safe and effective method of thermally actuating various device geometries *in vivo*. A novel scheme of actuation by Curie-thermoregulated inductive heating is presented. Prototype medical devices made from SMP loaded with nickel zinc ferrite ferromagnetic particles were actuated in air by applying an alternating magnetic field to induce heating. Dynamic mechanical thermal analysis was performed on both the particle-loaded and neat SMP materials to assess the impact of the ferrite particles on the mechanical properties of the samples. Calorimetry was used to quantify the rate of heat generation as a function of particle size and volumetric loading of ferrite particles in the SMP. These tests demonstrated the feasibility of SMP actuation by inductive heating. Rapid and uniform heating was achieved in complex device geometries and particle loading up to 10% volume content did not interfere with the shape recovery of the SMP.**

Index Terms—**Curie temperature, inductive heating magnetic particle, medical device, shape memory polymer (SMP).**

I. INTRODUCTION

SHAPE MEMORY POLYMERs (SMPs) are a class of polymeric materials that can be formed into a specific primary shape, reformed into a stable secondary shape, and then controllably actuated to recover the primary shape. A review of SMP basics and representative polymers was given by Lendlein [1]. The majority of SMPs are actuated thermally, by raising the temperature of the polymer above the glass (or crystalline) transition of the matrix phase. Typically, through this transition the modulus decreases from that characteristic of the glassy state ($\sim 10^9$ Pa) to that of an elastomer ($\sim 10^6$–10^7 Pa). Upon cooling, the original modulus is almost completely recovered and the primary form is stabilized. While other classes of thermally activated shape memory materials have been developed, shape memory alloys (SMA) [2] and shape memory ceramics [3] being the two other major classes [4], SMPs have a number of unique and promising properties. Specifically, in the field of medicine, research into the development of new SMP with adjustable modulus [5], greater strain recovery, an adjustable actuation temperature, and the option of bioresorption [1], [6] has opened the possibility for new medical devices and applications.

Some SMP devices that are being researched presently include an occlusive device for embolization in aneurysms [7], a microactuator for removing clots in ischemic stroke patients [8], [9], a variety of expandable stents with drug delivery mechanism [10], [11], cell seeded prosthetic valves [11], and self tensioning sutures [1]. One of the key challenges in realizing SMP medical devices is the design and implementation of a safe and effective method of thermally actuating a variety of device geometries *in vivo*. When the soft phase glass transition temperature of the SMP is above body temperature, an external heating mechanism, usually photothermal (laser heating) or electrical (resistive heating, or electric field) is required [8], [12]. A novel alternative to these methods of actuation is inductive heating: loading ferromagnetic particles into the SMP and exposing the doped SMP to an alternating magnetic field to cause heating.

The use of magnetic particles and an applied magnetic field has a variety of potential advantages over previous actuation methods. One of the key advantages is the innate thermoregulation offered by a ferromagnetic material's Curie temperature (T_c). T_c is the temperature at which a ferromagnetic material becomes paramagnetic, losing its ability to generate heat via a hysteresis loss mechanism [13]. By using particle sizes and materials that will heat mainly via a magnetic hysteresis loss mechanism instead of an eddy current mechanism, it becomes possible to have an innate thermoregulation mechanism that limits the maximum achievable temperature to T_c. By selecting a ferromagnetic particle material with a T_c within safe medical limits, Curie thermoregulation eliminates the danger of overheating and the need for a feedback system to monitor device temperatures. Other benefits of the inductive heating approach are the following.

1) Power transmission lines leading to a SMP device are eliminated. Eliminating fiber optics and wires and the connection of these items to a device simplifies design and eliminates a possible point of failure.
2) More complex device shapes are possible. Provided that uniform distribution of the magnetic particles is achieved, the conduction lengths are short and consistent heating is expected for any type of device geometry, whereas traditional laser and electro-resistive heating methods impose

*P. R. Buckley is with the Lawrence Livermore National Laboratory, Livermore, CA 94550 USA (e-mail: buckley@alum.mit.edu).

G. H. McKinley is with the Massachusetts Institute of Technology, Cambridge, MA 02139 USA (e-mail: gareth@mit.edu).

T. S. Wilson, W. Small, IV, W. J. Benett, J. P. Bearinger, M. W. McElfresh, and D. J. Maitland are with the Lawrence Livermore National Laboratory, Livermore, CA 94550 USA (e-mail: wilson97@llnl.gov; small3@llnl.gov; benett1@llnl.gov; bearinger1@llnl.gov; mcelfresh@llnl.gov; maitland1@llnl.gov).

constraints on device geometry due to the requirement of correct light refraction/absorption and thermal conduction through the device geometry.

3) Selective heating of specific device areas is possible by impregnating only the desired areas with magnetic particles. This scheme, in effect, allows a device to have a variable modulus from location to location in the device, introducing a new design variable and the possibility for new types of devices.

4) Remote actuation allows for the possibility of implantable devices that can be later actuated by an externally applied magnetic field, opening the possibility for an entirely new class of SMP devices such as tissue scaffolds for tissue regeneration.

The use of medically safe magnetic fields to selectively heat Curie thermoregulated ferromagnetic materials *in vivo* to temperatures of $\geq 42\,°C$, has been demonstrated in a number of hyperthermia studies [14]–[19] suggesting the feasibility of the same approach to actuate SMP devices *in vivo*. The impact of particle size and material processing on the magnetic loss mechanisms and heating characteristics of magnetic particles is quite complicated but is fairly well understood thanks to previous research [20], [21]. Theories have been developed that allow analytical techniques to optimize particle size and processing to maximize heating for a specified amplitude and frequency magnetic field [22], [23]. In fact, particle sizing and material processing to optimize heating characteristics in medically safe magnetic fields for biocompatible magnetite materials has already been laid out in research done on magnetic fluid hyperthermia (MFH) [20], [22], [24]. If anything, these previously reported magnetite particles heating efficiencies are overly optimized for an SMP application as it will be possible to have higher concentrations of particles in the SMP than it is possible to achieve in cancerous cells, which must be enticed to take up the particles and are only expected to have particle concentrations of roughly 15 mg Fe/g [25]. Unfortunately, these magnetite-based MFH particles that have been optimized for heating efficiency are not optimized for Curie thermoregulation, which is a desired property for particles used in an SMP application. Materials tailored to have a Curie temperature in the physiologically useful range have been developed [26], but are often less biocompatible then the magnetite materials previously mentioned. The biocompatibility requirements for the proposed SMP application require further investigation.

In this work, nickel zinc ferrite particles were used to achieve SMP actuation by inductive heating. Prototype SMP medical devices made from nickel zinc ferrite loaded SMP were thermally actuated in air using a 12.2 MHz magnetic field to demonstrate feasibility of the inductive heating approach. The effect of volumetric particle loading from 1% to 20% on the heating efficiency of the magnetic particles was also investigated. Dynamic mechanical thermal analysis (DMTA) was used to assess the change in mechanical properties of the SMP with the addition of particles at 10% volume content.

II. MATERIALS AND METHODS

A. Magnetic Particles

Nickel zinc ferrites are one class of material that shows promise for an inductively heated SMP application. Research
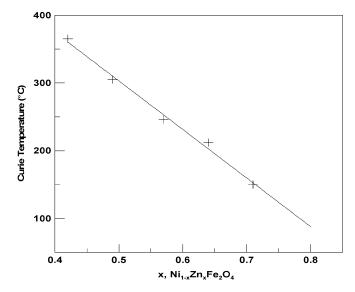

Fig. 1. Effect of Zn substitution on the Curie temperature of NiZn ferrite [27].

into the use of inductively heated particles for the bonding and curing of thermoplastics has already demonstrated that nickel zinc ferrites can have variable Curie temperature through zinc substitution, as shown in Fig. 1, as well as the ability to achieve self-thermoregulation via a Curie hysteresis mechanism [27]. Besides having an adjustable Curie temperature, nickel zinc ferrites have other material properties that make them well-suited to the proposed SMP application. They have a high electrical resistivity, on the order of 10^6–10^{10} Ohm-cm, this serves to minimize eddy current heating [27] allowing heat to be generated mainly via hysteresis losses. They are also environmentally stable, making it less likely that the particles will react with the polymer material.

Three compositions of nickel zinc ferrites were obtained from Ceramic Magnetics, Inc.: C2050, CMD5005, and N40. This nomenclature is provided by the manufacturer and does not indicate any specific material composition or concentration. These particles were reported by the manufacturer to have an average size of roughly 50 μm and a spherical shape. Particles were sorted further using 53, 43, 25, 16, and 8 μm pore screen meshes and some material was also ball-milled to obtain even smaller particles. Image analysis was used to classify particle size. Three different average sizes were obtained: 43.6, 15.4, and 6.7 μm. The 6.7 μm particles were produced from a 5 h ball milling process. Pertinent properties of these materials, including Curie temperature, are listed in Table I.

B. Magnetic Field Generation

The induction heating equipment used for initial testing was an Ameritherm Nova 1M power supply with a remote heat station, and a copper-wound solenoid coil with a 2.54 cm diameter, 7.62 cm length, and a total of 7.5 turns. This unit had an adjustable power setting capable of outputting 27–1500 Watts at between 10 and 15 MHz frequency. This high frequency would likely induce eddy currents in tissue .[14], causing undesirable direct heating of the human body in medical applications. While the high frequencies used here are not suitable for direct clinical use, the same magnetic loss mechanisms present at the clinically

TABLE I
MAGNETIC AND MATERIAL PROPERTIES OF NICKEL ZINC FERRITE PARTICLES

	C2050	CMD5005	N40
Initial Permeability	100	1600	15
Max Permeability	390	4500	50
Max Flux Density* (Gauss)	3400	3000	1600
Remnant Flux Density* (Gauss)	2400	1800	700
Coercive Force* (A/m)	239	18	597
Curie Temperature (°C)	340	130	510
Density (g/cm³) †	5.57	6.16	5.65
Resistivity (Ohm-cm)	10^6	10^9	10^{10}

*Measurement reported by manufacturer at 3184 A/m applied field strength
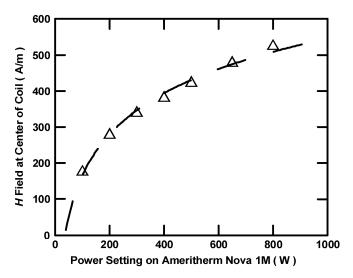†Measurement made by authors (not provided by manufacturer)

Fig. 2. Calibration curve (log fit to calculated data points) showing magnetic field generated at given power setting on Ameritherm Nova 1 M equipment.
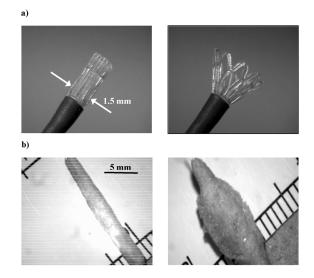

Fig. 3. SMP devices used to evaluate feasibility of actuation by inductive heating. a) Flower shaped device shown in collapsed and actuated form. b) SMP foam device shown in collapsed and actuated form.

usable frequencies, 50–100 kHz [28], should also be present in the particle materials at the higher frequencies used here, albeit at a different quantitative level. For these reasons, the 10–15 MHz range was seen as suitable for proof-of-principle testing.

The magnetic field was calculated indirectly using measurements of the impedance and the voltage drop across the coil. A Hewlett Packard 4285A 75 kHz–30 MHz LCR meter was employed to measure the impedance, which was (525 ± 7.2) nH at a frequency of 12.96 MHz. Assuming that the electrical resistance of the copper coil was negligible compared with the resistance created by the inductive reactance, it becomes possible to calculate the current through the coil using the following equations:

$$2\pi f L = X_L \qquad (1)$$
$$\frac{V}{X_L} = i \qquad (2)$$

where L is the impedance in Henry (525 nH), f is the frequency in Hz as measured using an oscilloscope, X_L is the inductive reactance, V is the rms voltage in volts as measured using an oscilloscope, and i is the calculated current in amps. Assuming the coil can be modeled as an ideal solenoid, the magnetic field at the center of the coil can be described as follows according to the Biot–Savart law [29]:

$$\frac{\mu_\circ N i}{\sqrt{(4R^2 + L^2)}} \times \frac{10^7}{4\pi} = H \qquad (3)$$

where $\mu_\circ$ is the permeability of free space and is equal to $4\pi \times 10^{-7}$ Henry/meter, N is the number of turns in the coil, i is the current through the coil in amps, R is the coil radius in meters, L is the coil length in meters, $(10^7)/(4\pi)$ is a conversion factor, converting from units of Tesla to A/m, and H is the field strength in A/m. Using the above techniques the peak magnetic field strength at the center of the coil was calculated for several power settings, this information is presented in the calibration curve found in Fig. 2. This calibration curve is not linear due

to the reflected power in the circuitry of the Ameritherm equipment [30].

C. Prototype Device

To determine the impact of the added magnetic particles on SMP shape recovery, a proof-of-principle test was conducted to evaluate the actuation of complex shaped devices made using ferromagnetic particle loaded SMP. Two prototype therapeutic devices currently being developed in-house that would be difficult to heat and actuate using laser or resistive heating techniques due to their complex geometries were chosen: a flower-shaped endovascular thrombectomy device for stroke treatment and an expandable SMP foam device for aneurysm embolization. These devices are shown in their collapsed and deployed forms in Fig. 3. These devices and mechanical test samples were made from an ester-based thermoset polyurethane SMP, MP 5510, purchased from Diaplex Company, Ltd., a subsidiary of Mitsubishi Heavy Industries, Ltd. The Diaplex SMPs

are segmented polyurethanes whose morphological structure is biphasic, consisting of a soft phase matrix with hard phase inclusions. Actuation is achieved by heating above the soft phase transition; the nominal soft phase glass transition temperature of MP 5510 is 55 °C. The SMP was loaded with 10% by volume C2050 43.6 μm diameter nickel zinc ferrite particles. The devices were exposed to an alternating magnetic field of 12.2 MHz and approximately 400 A/m (center of the inductive coil) in air at room temperature while an infra-red thermal imaging camera recorded device temperature during actuation.

D. Dynamic Mechanical Thermal Analysis (DMTA)

To quantify the impact of the nickel zinc ferrite particles on the mechanical properties of the SMP, a DMTA test was conducted on neat SMP and particle loaded SMP. Testing samples were prepared using the same SMP, particles, and particle concentrations used in the prototype devices previously described. Measurements were made using a TA ARES-LS2 model rheometer with TA Orchestrator control software. The test atmosphere was dry air with heating by forced convection. Samples were first prepared by polymerizing in 1 ml syringes (polypropylene) at manufacturer recommended conditions [31]. Resulting samples were typically 4.65 mm in diameter and up to 70 mm in length. The ARES instrument was set up with a torsion cylinder test fixture and the test geometry typically used was at the molded diameter and with a 25 mm gap between upper and lower fixtures. Dynamic strain sweeps at temperature extremes (25 °C and 120 °C) were used to determine the range of linear viscoelastic behavior of the neat polymer. Dynamic temperature sweep tests were then performed on all samples at 6.28 rad/s (1 Hz) frequency from 25 °C to 120 °C, at a constant heating rate of 1 °C/min, and starting with a shear strain of 0.01%, while using the control features of the software to adjust strain upward as temperature increased to maintain a minimum torque of 2 gram-cm. Data points were collected every 15 s. The rheological quantities of dynamic shear storage modulus G', dynamic shear loss modulus G", and the loss ratio $\tan \delta (= \text{G"/G'})$ were calculated by the Orchestrator software from the raw torque and angular displacement data using standard formulae [32].

E. Curie Thermoregulation and Hysteresis Loss

The presence of eddy current loss mechanisms in the inductive heating process can overcome the mechanism of thermoregulation offered by the Curie temperature limit imposed by hysteresis loss. Therefore, if temperatures above the particle Curie temperature can be reached in a given applied magnetic field, eddy current loss exists. The presence of eddy current loss was determined by using flakes of various Omega Marker temperature sensitive waxes mixed with the nickel zinc ferrite particles and then heated in a 12.2 MHz 545 A/m magnetic field. The thermo-sensitive wax transitions rapidly from a solid to a liquid at a prescribed temperature making it possible to determine when the particles had reached a specific temperature by physical observation.
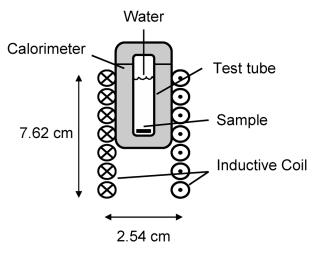

Fig. 4. Calorimeter test setup with inductive coil specifications.

F. Calorimetry Tests

A calorimeter was made using a 2.54 cm diameter styrofoam cylinder. A 1.27 cm hole was bored through the center of the styrofoam to accommodate a 1.27 cm diameter plastic test tube filled with 4 ml of double distilled deionized water. A styrofoam top was fashioned to cover the exposed top of the test tube. This testing setup is illustrated in Fig. 4. This configuration left a 6.35-mm-thick wall of insulating styrofoam around the entire test tube. To check that this was sufficient to prevent discernable heat loss to the environment a heat transfer calculation for the calorimeter geometry was conducted. The convective heat transfer coefficient for the calorimeter geometry of the calorimeter with free air convection was calculated to be $h = 4.507$ W/m^{2}K. Using this value, the time for the system to reach 95% of its steady-state temperature, meaning the inflow of heat is approximately equal to the outflow, was calculated to be 464.4 s. This value is an order of magnitude greater than the time of the longest test, which was 45 s, suggesting that heat loss over the course of the tests was negligible.

SMP calorimetry samples were 1-mm-thick discs with a diameter of 9.52 mm. Twelve different MP 5510 SMP samples with varying magnetic particle sizes, volume content, and material types were prepared and tested. A SMP disc of the same geometry as the other samples but with no magnetic particles was also tested to serve as a control.

Samples were loaded into the styrofoam calorimeter so they were centered in the inductive coil. The sample position in the coil was consistent for all tests to ensure that all samples experienced the same magnetic field. An alternating magnetic field of 12.2 MHz and prescribed field strength was then applied for a designated amount of time. Immediately after the field was turned off, the temperature rise of the water was measured using a thermocouple. Temperature was not measured during magnetic field exposure because the thermocouple would have been directly heated by the magnetic fields used.

Tests were performed at a power setting of 500 and 1000 Watts on the Ameritherm power supply, and at 10, 20, 30, and 45 s exposure times. These power settings correspond to peak field strengths of (422 ± 35) A/m and (545 ± 45) A/m as calculated using (1)–(3) (see calibration curve in Fig. 2).
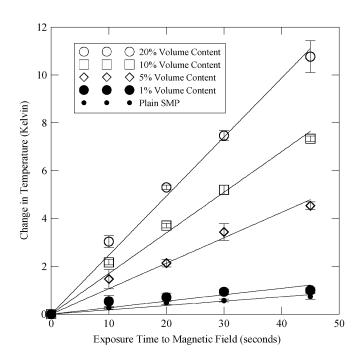
Fig. 5. Heating curves of SMP loaded with 43.6 μm C2050 particles at varying volume contents with error bars at $\pm$ one standard deviation. The slope of each curve was used to calculate the power dissipation.

Temporal heating curves (temperature change as a function of magnetic field exposure time) were generated by averaging three temperature measurements for the same samples at each time setting, a representative set of these curves is shown in Fig. 5.

Using the temperature rise measured in this series of tests, a power dissipation rate for each sample was calculated. It was assumed that the mass of the sample disc had negligible effect on the thermal properties of the system since the sample disc was less than 3%, by mass or volume, of the 4 ml of water. Using this assumption and neglecting any heat loss to the environment, the power generated in each test is equal to the power needed to heat the 4 ml of water. This allows the power dissipation to be calculated using the following equation:

$$\rho_w C_p v_w \frac{dT}{dt} = P_g \qquad (4)$$

where ρ_w is the density of water in units of g/cm^3 (0.99823 g/cm^3), c_p is the specific heat of water in units of J/gK (4.182 J/gK), v_w is the volume of water in units of cm^3 (4 cm^3), dT/dt is the rate of temperature rise of the water in units of K/s (calculated from the slope of the heating curves), and P_g is the dissipation in Watts. P_g was divided by the sample volume, 0.07118 cm^3, to derive the average volumetric power dissipation of the inductively heated SMP samples. The volumetric power dissipation of the magnetic particles was also calculated by first subtracting the P_g of the neat SMP control sample from that of the particle loaded samples, and then dividing this adjusted P_g by the volume of the magnetic particles.
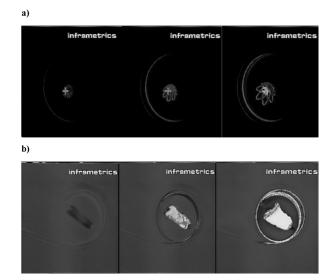

Fig. 6. a) Actuation of SMP flower shaped device with 10% volume fraction of 43.6 μm particle diameter C2050 magnetic material (12.2 MHz at 400 A/m applied magnetic field). b) Actuation of SMP foam with 10% volume fraction of 43.6 μm particle diameter C2050 magnetic material (12.2 MHz at 400 A/m applied magnetic field).

III. RESULTS

A. Prototype Device Actuation

Thermal images of the SMP devices actuating are shown in Fig. 6. Both the flower and foam devices fully actuated, showing qualitatively that the presence of particles up to 10% by volume did not interfere with the shape memory properties of the material. The flower actuated in under 25 s, with the magnetic field elevating the temperature of the device from 23 °C to 64 °C. The foam actuated in under 15 s with the temperature rising from 23°C to over 78.6 °C. Neither particle volume content nor magnetic materials were optimized for either of the devices.

B. Dynamic Mechanical Thermal Analysis (DMTA)

The glass transition temperature of the SMP and the ratio of glass state to rubber plateau moduli have been used previously to characterize the SMP actuation temperature and shape recovery properties of SMPs [33], [34]. DMTA was used to determine these properties for particle-loaded and neat (unloaded) SMP, with storage and loss moduli G' and G" shown in Fig. 7. Values of Tg, as well as the storage moduli (G') at T_g−20 °C, and at T_g+20 °C were calculated from the data and are given in Table II. While either the peak in G" or the peak in $\tan\delta$ are often used to define Tg, the average temperature of the two peaks is used to determine Tg here, with the following justification. The average in peak temperature is closer to the midpoint in the transition from the glassy state modulus to the rubber plateau modulus for these materials. The maximum in loss modulus and $\tan\delta$ that occur during DMTA tests signal different degrees of molecular motion in the polymer, with the maximum in the loss modulus signaling shorter range motion associated with the onset of the glass transition region, and the maximum in $\tan\delta$ signaling longer range coordinated molecular motion
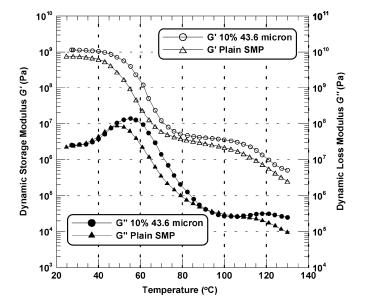
Fig. 7. DMTA results for neat SMP and a 10% volume fraction of 43.6 μm particle diameter C2050 magnetic material SMP sample.

Fig. 8. Volumetric power dissipation of magnetic particles versus volume fraction of particles, 12.2 MHz and 545 A/m.

TABLE II
DMTA RESULTS FOR PARTICLE LOADED SMP COMPARED
WITH NEAT (UNLOADED) SMP

Volume (%), Particle Diameter (μm), Material	G'(Tg-20C) (MPa)	G'(Tg+20C) (MPa)	T$_g$ (°C)
10%, 43.6μm, C2050	1010	4.85	61.4
0%, neat SMP	646	3.09	55.5

associated with approaching the end of the glass transition region and the beginning of the rubbery plateau region [34]. In the case of SMPs, it has been found that the temperature at which recovered strain increases with temperature is maximum near the midpoint in the modulus curve and below the Tg as determined by $\tan \delta$ [35]. We have found that as applied to SMPs choosing the Tg to be the average of T(G" peak) and T ($\tan \delta$) maximum defines well the actuation transition, and it is thus used here. All of these values increased with the addition of particles.

C. Curie Thermoregulation

Using the thermosensitive waxes to gauge the temperature of the nickel zinc ferrite particles, CMD5005 and C2050 were observed to stop heating at close to their nominal Curie temperatures of 130 °C and 340 °C, respectively. The Curie temperature of N40 (510 °C) was beyond the temperature range of the Omega Marker waxes but it was observed to heat above 340 °C as expected. While these temperatures may exceed acceptable physiological limits, the results demonstrate the nature of Curie thermoregulation, and they suggest that the magnetic heating mechanisms at work are those of hysteresis losses and not eddy currents at the applied field of 12.2 MHz and 545 A/m. Further, theoretical predictions of eddy current power dissipation in conductive particles show a direct proportionality with the square of the frequency of the applied field and the diameter of the particle [36], suggesting that the use of lower frequencies and smaller particles would even further reduce the presence
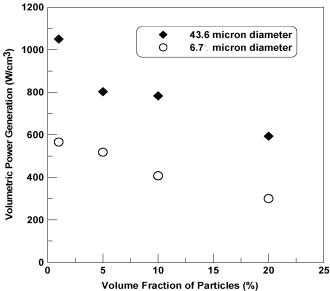
of eddy currents, thereby maintaining and even enhancing the Curie thermoregulation mechanism.

D. Calorimetry Tests

Representative temporal heating curves for SMP loaded with a specific particle type and size (C2050, 43.6 μm), as well as for neat (unloaded) SMP are shown in Fig. 5. Volumetric power dissipation of nickel zinc ferrite particles between 6.7–43.6 μm diameter was demonstrated to be between 128-1050 W/cm^3 for a 12.2 MHz magnetic field strength of 422–545 A/m, as shown in Table III. The observed decrease in power dissipation as particle diameter decreased was a predictable result according to multidomain magnetic particle theory that shows coercivity to be proportional to the inverse of the diameter [22]. Also, basic magnetic hysteresis theory predicts the observed increase in power dissipation for multidomain magnetic particles at increasing magnetic field strengths when field amplitudes are below the material coercivity [37], as is the case in these tests. An interesting and unexpected trend that is present in the calorimetry data is a decrease in the particle heating efficiency as the volume content of particles increases. This trend was present for both field strengths, 545 and 422 A/m, and can be seen in the 545 A/m data in Fig. 8. The volumetric power dissipation of the magnetic particles in SMP at 20% volume fraction was roughly 40% less than that at 1% volume fraction.

IV. DISCUSSION

While the high Curie temperature of the magnetic particles and frequency of the magnetic fields used here are not optimized for medical use, clinically safe magnetic fields have been used to selectively heat Curie thermoregulated ferromagnetic materials *in vivo* to clinically relevant temperatures of ≥ 42 °C in a number of hyperthermia studies [14]–[19], suggesting the feasibility of the same approach to actuate SMP devices *in vivo*. For these reasons, it should be easy to find a suitable particle material that heat with clinically safe magnetic fields. However,

TABLE III
VOLUMETRIC POWER DISSIPATION OF MAGNETIC PARTICLES AND AVERAGE VOLUMETRIC POWER DISSIPATION OF SAMPLES
FOR 12.2 MHz AND 422 AND 545 A/m MAGNETIC FIELDS

Magnetic Material	Volume %, Particle Diameter	Volumetric Power Dissipation of Magnetic Particles (W/cm^3)		Average Volumetric Power Dissipation of Samples (W/cm^3)	
		422 A/m Field	545 A/m Field	422 A/m Field	545 A/m Field
C2050	1, 6.7 μm	208	566	2.1	5.7
C2050	1, 43.6 μm	500	1050	5.0	10.5
C2050	5, 6.7 μm	240	518	12.0	25.9
C2050	5, 43.6 μm	414	803	20.7	40.1
C2050	10, 6.7 μm	177	407	17.7	40.7
C2050	10, 15.4 μm	338	717	33.8	71.7
C2050	10, 43.6 μm	356	783	35.6	78.3
C2050	20, 6.7 μm	128	300	25.6	60.0
C2050	20, 43.6 μm	268	593	53.6	118.6
N40	10, 43.6 μm	278	495	27.8	49.5
CMD5005	10, 43.6 μm	296	503	29.6	50.3
None (neat SMP)	N/A	N/A	N/A	4.0	6.0

questions about how particles interact with the SMP matrix and how their dispersion and proximity to one another affect heating characteristics remain.

The observed decrease in the volumetric heating efficiency of particles as volume content of particles in SMP increased points to a possible magnetic shielding effect the particles may have on each other as they become more closely packed in the polymer matrix. This shielding could lower the magnetic field strength experienced by the particles, and thus lower the volumetric power dissipation. No previous research on this effect has been found, making it a possible topic for further work. While the diminished heating efficiency of particles at higher volume content is something to be aware of, it does not appear that it will prevent SMP actuation as sufficient heating for SMP actuation occurred at relatively low particle concentrations of 5%–10% by volume.

The effect of particulate filler on a continuous polymer matrix has been previously studied in great detail and a number of models exists which can predict the impact of particles on the shear modulus of the composite [38]. The DMTA results can be compared with these theoretical predictions in order to provide a sense of how closely the inductively heated SMP materials conform to classical expectations. One well-known model is the Guth and Smallwood equation, which is an extension of the Einstein equation to include two particle interactions [38]

$$G = G_m(1 + 2.5\phi + 14.1\phi^2) \qquad (5)$$

where G is the shear modulus of the polymer/particle composite, G_m is the matrix modulus taken to be that of the neat polymer, and ϕ is the volume fraction of particles. Equation (5) predicts that the presence of 10% volume of particles should increase the modulus by roughly 39%. The observed results were close to this, with the glassy modulus of the material increasing by 56%, and the rubbery modulus by 24%. More extensive DMTA testing is in progress to further characterize the

affect that different particle volume contents have on the mechanical properties of the SMP. More information on the impact of particle loading on the mechanical properties of SMP particle composites can be found in previous research [39], [40]

V. CONCLUSION

We have demonstrated the feasibility of fabricating inductively heated SMP devices employing dispersed nickel zinc ferrite ferromagnetic particles and using a magnetic field to trigger actuation. Elimination of a physical power connection removes restrictions on device geometry imposed by laser and resistive heating modalities. Furthermore, as a result of the predominant hysteresis loss heating mechanism, self-thermoregulation can be achieved by tailoring the particle Curie temperature to prevent overheating in medical applications. Initial actuation testing indicated that the addition of 10% volume content of particles provides sufficient heating for SMP actuation in air and does not interfere significantly with the shape memory properties of the material. Preliminary DMTA results show an increase in the modulus of the SMP composite with the addition of 10% particles that is in accordance with standard composite theory, as well as an increase in the glass transition temperature of the soft phase of the SMP. With further optimization of particle material to provide clinically acceptable Curie temperatures and magnetic field frequencies, inductive heating may provide an effective means of deployment of SMP medical devices.

REFERENCES

[1] A. Lendlein and R. Langer, "Biodegradable, elastic shape-memory polymers for potential biomedical applications," *Science*, vol. 296, pp. 1673–1676, 2002.
[2] L. M. Schetky, "Shape memory alloys," *Scientific Amer.*, vol. 241, pp. 74–82, 1979.
[3] M. V. Swain, "Shape memory behavior in partially-stabilized zirconia ceramics," *Nature*, vol. 322, pp. 234–236, 1986.
[4] K. Otsuka and C. M. Wayman, *Shape Memory Materials*. Cambridge, U.K.: Cambridge Univ. Press, 1998.
[5] Y. Liu, K. Gall, M. L. Dunn, P. McCluskey, and R. Shandas, "Shape memory polymers for medical applications," *Adv. Mater. Process.*, vol. 161, p. 31, 2003.

[6] M. Bertmer, A. Buda, I. Blomenkamp-Hofges, S. Kelch, and A. Lendlein, "Biodegradable shape-memory polymer networks: Characterization with solid-state NMR," *Macromolecules*, vol. 38, pp. 3793–3799, 2005.

[7] A. Metcalfe, A.-C. Desfaits, I. Salazkin, L. H. Yahia, W. M. Sokolowski, and J. Raymond, "Cold hibernated elastic memory foams for endovascular interventions," *Biomaterials*, vol. 24, p. 491, 2003.

[8] D. J. Maitland, M. F. Metzger, D. Schumann, A. Lee, and T. S. Wilson, "Photothermal properties of shape memory polymer micro-actuators for treating stroke," *Lasers in Surgery and Medicine*, vol. 30, pp. 1–11, 2002.

[9] M. F. Metzger, T. S. Wilson, D. Schumann, D. L. Matthews, and D. J. Maitland, "Mechanical properties of mechanical actuator for treating ischemic stroke," *Biomedical Microdevices*, vol. 4, pp. 89–96, 2002.

[10] H. M. Wache, D. J. Tartakowska, A. Hentrich, and M. H. Wagner, "Development of a polymer stent with shape memory effect as a drug delivery system," *J. Mater. Sci.: Mater. in Medicine*, vol. 14, p. 109, 2003.

[11] K. Gall, C. M. Yakacki, Y. Liu, R. Shandas, N. Willett, and K. S. Anseth, "Thermomechanics of the shape memory effect in polymers for biomedical applications," *J. Biomed. Mater. Res.—Part A*, vol. 73, p. 339, 2005.

[12] Y. C. Jung, N. S. Goo, and J. W. Cho, "Electrically conducting shape memory polymer composites for electroactive actuator," presented at the Proc. Smart Structures and Mater. 2004: Electroactive Polymer Actuators and Devices (EAPAD), San Diego, CA, 2004.

[13] A. Goldman, *Modern Ferrite Technology*. New York: Van Nostrand Reinhold, 1990.

[14] P. Stauffer, T. Cetas, A. Fletcher, D. DeYoung, M. Dewhirst, J. Oleson, and R. Roemer, "Observations on the use of ferromagnetic implants for inducing hyperthermia," *IEEE Trans. Biomed. Eng.*, vol. 31, pp. 76–90, 1984.

[15] T. C. Cetas, E. J. Gross, and Y. Contractor, "A ferrite core/metallic sheath thermoseed for interstitial thermal therapies," *IEEE Trans. Biomed. Eng.*, vol. 45, no. 1, pp. 68–77, Jan. 1998.

[16] A. Jordan, P. Wust, H. Fahling, W. John, A. Hinz, and R. Felix, "Inductive heating of ferrimagnetic particles and magnetic fluids: Physical evaluation of their potential for hyperthermia," *Int. J.Hyperthermia: The Official J. Eur. Soc. Hyperthermic Oncology, North American Hyperthermia Group*, vol. 9, pp. 51–68, 1993.

[17] W. Atkinson, I. Brezovich, and D. Chakraborty, "Usable frequencies in hyperthermia with thermal seeds," *IEEE Trans. Biomed. Eng.*, vol. 31, pp. 70–75, 1984.

[18] J. A. Paulus and R. D. Tucker, "Cobalt palladium seeds for thermal treatment of tumors patent," U.S. 5429583, Jul. 4, 1995.

[19] N. Ramachandran and K. Mazuruk, "Magnetic microspheres and tissue model studies for therapeutic applications," *Transport Phenomena In Microgravity, Annals of The New York Academy of Sciences*, vol. 1027, pp. 99–109, 2004.

[20] R. Hergt, W. Andra, C. d'Ambly, I. Hilger, W. Kaiser, U. Richter, and H.-G. Schmidt, "Physical limits of hyperthermia using magnetite fine particles," *IEEE Trans. Magn.*, vol. 34, no. 5, pp. 3745–3754, Sep. 1998.

[21] A. E. Virden and K. O'Grady, "Structure and magnetic properties of NiZn ferrite nanoparticles," *J. Magn. Magn. Mater.*, vol. 290, pp. 868–870, 2005.

[22] M. Ma, Y. Wu, J. Zhou, Y. Sun, Y. Zhang, and N. Gu, "Size dependence of specific power absorbtion of Fe_3O_4 particles in AC magnetic field," *J. Magn. Magn. Mater.*, pp. 33–39, 2004.

[23] Gray, Cammarano, and Jones, "Heating of magnetic materials by hysteresis effects patent," U.S. us659923B1, Jul. 29, 2003.

[24] A. Jordan, R. Scholz, P. Wust, H. Fahling, and F. Roland, "Magnetic fluid hyperthermia (MFH):Cancer treatment with AC magnetic field induced excitation of biocompatible superparamagnetic nanoparticles," *J. Magn. Magn. Mater.*, pp. 413–419, 1999.

[25] A. Jordan, R. Scholz, K. Maier-Hauff, M. Johannsen, P. Wust, J. Nadobny, H. Schirra, H.-G. Schmidt, S. Deger, S. Loening, W. Lanksch, and R. Felix, "Presentation of a new magnetic field therapy system for the treatment of human solid tumors with magnetic fluid hyperthermia," *J. Magn. Magn. Mater.*, pp. 118–126, 2001.

[26] J. Giri, A. Ray, S. Dasgupta, D. Datta, and D. Bahadur, "Investigation on T-c tuned nano particles of magnetic oxides for hyperthermia applications," *Bio-Med. Mater. Eng.*, vol. 13, pp. 387–399, 2003.

[27] X. K. Zhang, Y. F. Li, J. Q. Xiao, and E. D. Wetzel, "Theoretical and experimental analysis of magnetic inductive heating in ferrite materials," *J. Appl. Phys.*, vol. 93, pp. 7124–7126, 2003.

[28] A. Jordan, R. Scholz, P. Wust, H. Fahling, and R. Felix, "Magnetic fluid hyperthermia (MFH): Cancer treatment with AC magnetic field induced excitation of biocompatible superparamagnetic nanoparticles," *J. Magn. Magn. Mater.*, vol. 201, pp. 413–419, 1999.

[29] V. Rudnev, *Handbook of Induction Heating*. New York: Marcel Dekker, 2003.

[30] Ameritherm, "Operation and maintenance instruction NovaStar 1M 10-15 MHz power supply," Ameritherm Inc., Scottsville, Doc # 801-9096 rC, 2000.

[31] M. H. I. Ltd, *Processing Instructions For Shape Memory Polymer (Manual No. 1 Rev. 2.2)*, 1992.

[32] C. W. Macosko, *Rheology: Principles, Measurements, and Applications*. New York: VCH, 1994.

[33] B. K. Kim, S. Y. Lee, and M. Xu, "Polyurethanes having shape memory effects," *Polymer*, vol. 37, pp. 5781–5793, 1996.

[34] L. H. Sperling, *Introduction to Physical Polymer Science*. New York: Wiley, 1986.

[35] J. R. Lin and L. W. Chen, "Shape-memorized crosslinked ester-type polyurethane and its mechanical viscoelastic model," *J. Appl. Polymer Sci.*, vol. 73, pp. 1305–1319, 1999.

[36] E. Wetzel and B. Fink, "Feasibility of magnetic particle films for curie temperature-controlled processing of composite materials," Army Res. Lab., Mar. 2001.

[37] C. Kittel, "Physical theory of ferromagnetic domains," *Rev. Mod. Phys.*, vol. 21, pp. 541–583, 1949.

[38] E. D. Bliznakov, C. C. White, and M. T. Shaw, "Mechanical properties of blends of HDPE and recycled urea-formaldehyde resin," *J. Appl. Polymer Sci.*, vol. 77, pp. 3320–3227, 2000.

[39] K. Gall, M. L. Dunn, Y. P. Liu, D. Finch, M. Lake, and N. A. Munshi, "Shape memory polymer nanocomposites," *Acta Materialia*, vol. 50, pp. 5115–5126, 2002.

[40] B. Yang, W. M. Huang, C. Li, L. Li, and J. H. Chor, "Qualitative separation of the effects of carbon nano-powder and moisture on the glass transition temperature of polyurethane shape memory polymer," *Scripta Materialia*, vol. 53, pp. 105–107, 2005.

Patrick R. Buckley received the B.S. degree in mechanical engineering and the M.S. degree from the Department of Mechanical Engineering, Massachusetts Institute of Technology (MIT), Cambridge, in 2003 and 2004, respectively.

Since Summer 2001, he has worked at the Lawrence Livermore National Laboratory (LLNL), Livermore, CA, when not in school. He has contributed to a wide variety of projects ranging from inertial fusion to MEMS biodetection devices, and finally, settling in the biomedical field.

Mr. Buckley was awarded the Sheriden Prize and the Wunsch Foundations Silent Hoist and Crane Award both for outstanding design while at MIT.

Gareth H. McKinley is Director of the Program in Polymer Science and Technology (PPST) at the Massachusetts Institute of Technology (MIT), Cambridge. He is also Director of the Hatsopoulos Microfluids Laboratory, Department of Mechanical Engineering, MIT. His research interests focus on the rheology and fluid dynamics of complex fluids and on the preparation and processing of nanocomposite materials. Current fluids of interest include polymer nanocomposites, field-responsive fluids, wormlike micellar solutions, polymer melts, nanoparticle suspensions, as well as foodstuffs such as bread dough, chocolate, and mayonnaise.

Thomas S. Wilson received the B.S. degree from the University of Wisconsin, Madison, in 1985 and the Ph.D. degree from Virginia Polytechnic Institute and State University, Blacksburg, in 1991, both in chemical engineering.

From 1991 to 2000, he was with Rohm and Hass Company, where he focused on the characterization of rheological, thermal, and physical properties of polymeric materials with application to new material development and material processing. Since 2000, he has worked in the Medical Physics and Biophysics Division at Lawrence Livermore National Laboratory (LLNL), Livermore, CA. His current research interests include synthesis and characterization of new shape memory polymers, hydrogels, and biomaterials for medical devices, biosensors, and artificial organs.

Dr. Wilson is a member of the American Chemical Society, the Society of Plastics Engineers, and the Society of Rheology.

Ward Small, IV received the B.S. degree in engineering physics from the University of California, San Diego, in 1993 and the Ph.D. degree in engineering/applied science from the University of California, Davis, in 1998.

He conducted his graduate research in laser-tissue interaction and biomedical optical diagnostics as a Student Employee/Physicist in the Medical Technology Program at Lawrence Livermore National Laboratory (LLNL), Livermore, CA. From 1998 to 2003, he was a Scientist and Project Manager at Miravant Medical Technologies, where he investigated the use of light-activated photodynamic therapy drugs for treating ophthalmic and dermatologic diseases. He returned to LLNL in 2003 to join the Medical Physics and Biophysics Division, where he currently develops photomechanical and electromechanical actuators for therapeutic medical devices. He holds two patents for an optical temperature sensing system. He has authored 14 peer-reviewed journal articles and 24 conference proceedings articles and abstracts. His research interests include biomedical optics and endovascular device development.

Dr. Small received an R&D 100 Award from *R&D Magazine*.

William J. Benett received the A.S. degree in electronics engineering from Los Angeles Trade Technical College, Los Angeles, CA, in 1974.

He joined the Hughes Aircraft Company in 1974, where he worked in the High Power Chemical Laser Program. Since 1977, he has been with Lawrence Livermore National Laboratory (LLNL), Livermore, CA, where he has contributed to several programs. As a member of the Laser Division, he worked in the Isotope Separation Program, where he conducted research on dye and copper vapor lasers. In 1986, he became a member of the Diode Pumped Solid State Laser Group, where he worked on laser diode packaging. In 1994, he joined the Micro Technology Center, where he has been developing packaging techniques for micromechanical, electronic, and fluidic systems. He has also led the effort to develop portable and flow through PCR thermal-cyclers for biowarfare/terrorism agent detection. Currently, he provides interventional device design and fabrication expertise to the Medical Technology Program. He has coauthored numerous publications in a variety of technical areas and has 35 granted patents.

Jane P. Bearinger received the B.S. degree in biochemistry from Trinity College, Hartford, CT, in 1990, and the M.S. and Ph.D. degrees in biomedical engineering from Northwestern University, Evanston, IL, in 1997 and 2000, respectively.

From 1990 to 1993, she was a Chemist at Merck and Company, where she concentrated on natural products chemistry. She spent 2000 to 2002 in Switzerland as a Postdoctoral Fellow at ETH/University of Zurich in the Biomedical Engineering and Surface Science Laboratories of Jeffrey Hubbell and Marcus Textor. Since 2002, she has been with Lawrence Livermore National Laboratory (LLNL), Livermore, CA, where she has served as SCL of the Bioorganic Synthesis and Protein Engineering Group in the Chemical Biology and Nuclear Science Division of CMS. She has served as a Reviewer for the *Institute of Physics Journals*. She has authored 19 publications. Her current research interests include novel surface patterning methods, deterministic collection of proteins, microbes and cells, and shape memory polymer formulation and actuation.

Dr. Bearinger is a member of the National Institutes of Health, National Center for Research Resources Study Section.

Michael W. McElfresh received the B.S. degree in biochemistry from the University of California, Davis, in 1979, the M.S. degree in chemistry from Washington University, St. Louis, MO, in 1981, and the Ph.D. degree in chemistry from the University of California, San Diego, in 1988, while working in physics.

From 1985 to 1988, he was a graduate student at the Los Alamos National Laboratory, where he worked on the magnetic and magneto-transport properties of f-electron systems. From 1988 to 1990, he was a Postdoc at the IBM T. J. Watson Research Center, Yorktown Heights, NY, where he worked on magneto-optics and high-temperature superconductors. From 1990 to 2000, he was a Professor of Physics at Purdue University and was also the Assistant Director of the Midwest Superconductivity Consortium and Director of the Purdue Materials Consortium. Since 2000, he has been with Lawrence Livermore National Laboratory (LLNL), Livermore, CA, where he has served as Director of the Materials Research Institute and is now a Senior Scientist in the Chemistry and Materials Science Directorate. He has over 100 refereed publications. His current research interests include mechanical properties of materials including measuring the strength of single biological chemical bonds and the development of magneto-optically based sensor systems.

Dr. McElfresh has served as a Reviewer for *Physical Review B*, the IEEE TRANSACTIONS ON MAGNETICS, and other journals.

Duncan J. Maitland received the B.S. degree in electrical engineering and the M.S. degree in physics from Cleveland State University, Cleveland, OH, in 1985 and 1989, respectively, and the Ph.D. degree in bioengineering from Northwestern University, Evanston, IL, in 1995.

From 1985 to 1987, he was a Flight Control Systems Engineer at Goodyear Aerospace before joining NASA Glenn (formerly Lewis) Research Center, where he built and tested prototype fiber-optic sensors for aircraft engines until 1989. Since 1995, he has been with Lawrence Livermore National Laboratory (LLNL), Livermore, CA, where he has served as Group Leader of the Medical Technology Program and Associate Division Leader of the Medical Physics and Biophysics Division. He has 35 publications and 7 granted patents. His current research interests include therapeutic laser-tissue interactions, interventional endovascular device development, and vascular fluid dynamics and thermal transport.

Dr. Maitland is a member of the National Institutes of Health Bioengineering and Physiology Study Section. He has served as a Reviewer for *Applied Optics*, *Optics Letters*, *Journal of Biomedical Optics*, and *Lasers in Surgery and Medicine*.